



Dynamic cerebral autoregulation estimates derived from near infrared spectroscopy and transcranial Doppler are similar after correction for transit time and blood flow and blood volume oscillations

Jan Willem J Elting^{1,*}, Jeanette Tas^{1,*}, Marcel JH Aries^{2,3}, Marek Czosnyka^{3,4} and Natasha M Maurits¹

Abstract

We analysed mean arterial blood pressure, cerebral blood flow velocity, oxygenated haemoglobin and deoxygenated haemoglobin signals to estimate dynamic cerebral autoregulation. We compared macrovascular (mean arterial blood pressure-cerebral blood flow velocity) and microvascular (oxygenated haemoglobin-deoxygenated haemoglobin) dynamic cerebral autoregulation estimates during three different conditions: rest, mild hypocapnia and hypercapnia. Microvascular dynamic cerebral autoregulation estimates were created by introducing the constant time lag plus constant phase shift model, which enables correction for transit time, blood flow and blood volume oscillations (TT-BF/BV correction). After TT-BF/BV correction, a significant agreement between mean arterial blood pressure-cerebral blood flow velocity and oxygenated haemoglobin-deoxygenated haemoglobin phase differences in the low frequency band was found during rest (left: intraclass correlation=0.6, median phase difference 29.5° vs. 30.7°, right: intraclass correlation=0.56, median phase difference 32.6° vs. 39.8°) and mild hypocapnia (left: intraclass correlation=0.73, median phase difference 48.6° vs. 43.3°, right: intraclass correlation=0.70, median phase difference 52.1° vs. 61.8°). During hypercapnia, the mean transit time decreased and blood volume oscillations became much more prominent, except for very low frequencies. The transit time related to blood flow oscillations was remarkably stable during all conditions. We conclude that non-invasive microvascular dynamic cerebral autoregulation estimates are similar to macrovascular dynamic cerebral autoregulation estimates, after TT-BF/BV correction is applied. These findings may increase the feasibility of non-invasive continuous autoregulation monitoring and guided therapy in clinical situations.

Keywords

Dynamic cerebral autoregulation, transcranial Doppler, near infrared spectroscopy, group delay, microvascular transit time

Received 4 June 2018; Revised 27 August 2018; Accepted 17 September 2018

Introduction

Analysis of cerebral vasoregulation can be based on macrovascular or microvascular measurements. The standard for macrovascular measurements is mean arterial blood pressure (MABP) and cerebral blood flow velocity (CBFV), which can be used as input–output variables for transfer function analysis (TFA) to obtain estimates of dynamic cerebral autoregulation (DCA).^{1–3} To calculate cerebral microvascular characteristics, such as the capillary transit time, microvascular autoregulation

¹Department of Neurology, University Medical Center Groningen, Groningen, The Netherlands

²Department of Intensive Care, Maastricht University Medical Center, Maastricht, The Netherlands

³Brain Physics Group, Department of Clinical Neurosciences, Addenbrooke's Hospital, University of Cambridge, Cambridge, UK

⁴Institute of Electronic Systems, Warsaw University of Technology, Warsaw, Poland

*Both authors contributed equally to this work.

Corresponding author:

Jan Willem J Elting, Department of Neurology, University Medical Center Groningen, Hanzeplein 1, Groningen 9713GZ, The Netherlands.
Email: j.w.j.elting@umcg.nl

and changes in blood flow and blood volume,^{4,5} near infrared spectroscopy (NIRS) may be used. To achieve this, several mathematical models that describe the complex cerebral microvascular hemodynamics and tissue oxygenation in terms of NIRS variables, such as oxygenated haemoglobin (OxyHb), deoxygenated haemoglobin (HHb), total haemoglobin (totalHb) and oxygenation index, have been proposed.⁶⁻⁸ A logical next step is to combine macro- and microvascular measurements to create a more complete picture of the cerebral circulation.^{9,10} Comparisons between macrovascular- and microvascular-based estimates of cerebral autoregulation can be made to answer the question if these measurements are related, and if they capture features of the same physiological processes. The rationale for assuming a relation between macrovascular- and microvascular-based estimates of DCA is that for both methods cerebral arteriolar myogenic activity is assumed to be the main regulator (Figure S1 in Appendix 1). Therefore, the terms macrovascular and microvascular relate only to the measurement site and not to the presumed site of action of cerebral autoregulation.

Discrepancies between both types of DCA estimates have been reported,⁵ but direct comparisons between microvascular- and macrovascular-based DCA estimates with simultaneous measurements of all relevant variables have rarely been described.⁹⁻¹¹ If microvascular- and macrovascular-based estimates of DCA were similar, this would be of considerable practical importance, since the feasibility of non-invasive continuous autoregulation monitoring and guided therapy in clinical situations would certainly increase with easy to apply NIRS methodology.¹²

An important difference between the microvascular and macrovascular measurements is that microvascular measurements are part of a serial system, while macrovascular measurements can be viewed as a parallel system; except for frequencies in the autoregulation range, oscillations in MABP and CBFV arrive at their measurement sites simultaneously.³ For microvascular measurements, oscillations in HHb are delayed compared to OxyHb as a result of passage through the capillary network. This creates transit time effects, which are visible in the frequency domain as the linear phase difference trend phenomenon of group delay: a constant transit time produces a different phase difference between the input and output signal for different frequencies¹³ (see Appendix 1, Part 4 for an example). Another factor that may induce additional constant phase differences between OxyHb and HHb is the 'washout' phenomenon: during changes in blood flow, an increase in OxyHb will be matched by a concurrent decrease in HHb, which will induce a constant phase difference of 180° between OxyHb and HHb oscillations. By contrast, when blood volume changes, OxyHb and HHb changes

will be synchronous, which will create a 0° phase difference.^{14,15} Both transit time effects and effects of varying blood flow and blood volume oscillations are superimposed on phase differences induced by cerebral autoregulation. Without additional analysis, it may therefore be impossible to separate autoregulation effects from transit time effects and blood flow and blood volume effects. In the field of movement disorders, the group delay phenomenon has been used to estimate corticospinal conduction time by using a constant time lag plus constant phase shift model.^{16,17} A similar analysis strategy may aid the TFA of NIRS data; we assume that the constant time lag is equivalent to the microvascular transit time, and the constant phase shift is generated by the balance between blood flow and blood volume oscillations. By applying this model to the NIRS data, we correct the OxyHb-HHb phase difference for transit time and blood flow and blood volume oscillation induced effects, which *could* enable an unbiased estimation of DCA induced phase differences. From a frequency domain-based system analysis perspective, this is equivalent to converting the serial OxyHb-HHb system back to a parallel system (see Supplementary Data, Appendix 1, Part 1). This is why MABP-CBFV and OxyHb-HHb phase differences can be similar in theory, and this formed one of our main hypotheses.

In this study, we combined DCA measurements based on MABP and CBFV with simultaneous bilateral high-frequency NIRS measurements in healthy human participants. To facilitate the autoregulation analysis, it is helpful to include the response to stimuli with a known effect on DCA, like changes in CO₂. Hypercapnia is known to change the autoregulatory state to a less efficient level and may also decrease cerebral transit times, with concomitant increases in cerebral blood flow and blood volume as a result of the microvascular dilatation that is induced.¹⁸⁻²¹

We compared three different conditions: rest, mild hypocapnia and hypercapnia. Standard procedures for DCA assessment were used on MABP and CBFV, while the constant time lag plus constant phase shift model was applied to OxyHb and HHb. We evaluated three main hypotheses:

1. Uncorrected cerebral autoregulation estimates will be different for MABP-CBFV and OxyHb-HHb.
2. Transit time and the balance between cerebral blood flow and blood volume oscillations can be determined by applying the constant time lag plus constant phase shift model to NIRS data.
3. Transit time, blood flow and blood volume oscillations (TT-BF/BV) corrected cerebral autoregulation estimates based on microvascular measurements (OxyHb-HHb) are similar to macrovascular (MABP-CBFV) estimates of cerebral autoregulation.

Materials and methods

Measurement protocol

Fifteen healthy participants (three male; median age (range) 28 years (21–45)) volunteered for this study after providing informed consent. The measurement protocol was approved by the ethics committee of the University Medical Centre Groningen and was in accordance with the latest version of the Declaration of Helsinki. During the measurements participants lay supine in a 30° head up position. Bilateral 2 MHz Transcranial Doppler (TCD) transducers (Delica, Shenzhen, China) were placed over the transtemporal bone window to record CBFV in both middle cerebral arteries (MCA). The NIRS sensors (Portalite, Artinis Medical Systems, Elst, The Netherlands: <http://www.artinis.com/portalite/>) were placed bilaterally on the forehead to measure OxyHb, HHb and TotalHb ($\mu\text{mol/litre tissue}$). A lateral position on the forehead was chosen to ensure the measurement would be in brain tissue within the vascular territory of the MCA. An optode distance of 40 mm was used for this study. A Portapress device (Finapres Medical Systems, Amsterdam, The Netherlands) was placed on the middle finger to measure MABP and heart rate (HR) continuously. The end-tidal CO₂ concentration (ETCO₂) was measured by mask capnography, except during the 8% CO₂ inhalation (hypercapnia). The measurement protocol consisted of 5-minute periods of rest (REST), followed by cyclic deep breathing (DB; hypocapnia) and finally DB with 8% CO₂ (DBCO₂; hypercapnia) inhalation periods. During REST, further analysis with TFA was based on spontaneous oscillations in MABP, CBFV, OxyHb and HHb during normocapnia. The reason to use DB is two-fold: firstly, it will induce MABP oscillations at a higher amplitude than spontaneous MABP oscillations.²² Several studies have shown that reproducibility of the DCA measurements may be improved by using induced MABP oscillations.^{23–25} Secondly, DB will induce a mild degree of hypocapnia, which can be contrasted with hypercapnia. The participants had to follow audio instructions that included breathing cycles of 8, 10, 14 and 20 s, covering the frequency range of 0.05–0.125 Hz. This frequency range was chosen such that it would include the upper very low frequency (VLF) and low frequency (LF) ranges that are used for the determination of DCA parameters. Individual variations in the sequence of breathing cycles were implemented by changing the order of the breathing frequencies semi-randomly, to approximate the condition of naturally occurring spontaneous oscillations as closely as possible.

Cerebral autoregulation analysis without TT-BF/BV correction

The 250 Hz (TCD) and 50 Hz (NIRS) data were pre-processed online to generate beat-to-beat data, but high-frequency data were also captured and stored separately. Other processing steps were performed retrospectively. Artefacts were removed after visual inspection. Occasional spike artefacts occurred and were removed by linear interpolation. In two cases, major movement related artefact occurred during REST, but this was identified during measurement and was corrected for by extending the registration. The data were thereafter linearly interpolated to 10 Hz. The data were split into the different frequency bands: VLF (0.02–0.07 Hz), LF (0.07–0.2 Hz) and high frequency (HF: 0.2–0.5 Hz). Power spectral density estimates were performed using the Welch method (100 s epochs, 50% window overlap). The relationships between MABP and CBFV and between OxyHb and HHb were determined with TFA using the recommendations of the international Cerebral Autoregulation Research Network.¹ After computing the gain, phase and coherence, the phase results were corrected for phase wrap around by visually inspecting the phase plots for sudden large phase changes, and subsequently adding or subtracting 360°. To estimate mean effects, we also created grand average waveform plots by averaging the TFA results across all participants. For the TFA results, the averaging was done on the real and imaginary parts of the transfer function, separately, which were subsequently transformed back to gain and phase estimates. This is a standard procedure for creating averages of circular data.²⁶

Transit time and blood flow and blood volume oscillation estimates

Because autoregulation effects are minimal above 0.2 Hz, the transit time analysis was performed on the phase difference spectrum in the HF range (0.2–0.5 Hz). For this part of the analysis, we used the high-frequency data, after low pass filtering the data with a sixth-order zero phase butterworth filter with a cut off frequency of 0.5 Hz. This resulted in higher coherences and smaller confidence limits for the phase difference estimates in the HF band compared to the beat to beat data. This is important as the transit time analysis is based on the HF band data.

The constant time lag plus constant phase shift model states that the phase shift at a specific frequency f_j between two oscillations, x and y , is given as²⁷

$$\varphi(f_j)_{xy} = 360 \cdot t \cdot f_j + \theta \quad (1)$$

where t is the constant time lag (in seconds) and θ is the constant phase shift between them. Applying equation (1) to NIRS, t is equivalent to the transit time TT and can be calculated from a phase difference spectrum with a linear slope between frequency f_i and frequency f_j as¹⁶

$$TT = \frac{\varphi(f_i)xy - \varphi(f_j)xy}{(f_i - f_j).360} \quad (2)$$

With short TT , the slope is low, while with longer TT it will become steeper.

The constant phase shift θ is particularly relevant when considering OxyHb and HHb data: the well-known 'washout' effect will induce a constant phase shift of 180° between OxyHb and HHb oscillations. This effect will be present if blood flow oscillations are prominent. On the other hand, we assume the constant phase shift to be 0° if blood volume oscillations are dominant, as has been suggested previously.^{14,15} Although blood flow oscillations are usually dominant in brain tissue,²⁸ a mixture of both blood flow and blood volume oscillations may be present, as has been previously reported in the literature, which may result in a constant phase difference in between 0° and 180° .^{29,30} Figure 1 illustrates these effects on simulated data. These effects were further examined and quantified in a simulation experiment, the details of which can be found in Appendix 1, Parts 1 and 2. Importantly, these simulations show that the slope of the linear phase difference trend can change as a result of different transit times but also as a result of different percentages of blood flow and blood volume oscillations. However, with changing transit times and constant blood flow and blood volume oscillations, the Y-axis intercept of the linear phase trend will remain constant, while with different percentages of blood flow and blood volume oscillations but constant transit time, the X-axis intercept of the linear phase trend will remain constant (Figure 1, bottom row). On the basis of these results, one can deduce that the percentage of blood flow oscillations (%BF) can be estimated from the Y-axis intercept ($Y_{x=0}$) as:

$$\%BF = \frac{Y_{x=0}}{180} \cdot 100 \quad (3)$$

With an increasing percentage of blood volume oscillations, the 0-s transit time associated with blood volume changes will reduce the slope of the linear phase difference trend, but the X-axis intercept ($X_{y=0}$) will still be determined by the transit time associated with blood flow oscillations. The transit time associated with blood flow changes ($TT(BF)$) can be retrieved by drawing a line between the point $Y = 180$; $X = 0$ and the X-axis

intercept and determining its slope according to equation (2):

$$TT(BF) = \frac{180}{X_{y=0}.360} \quad (4)$$

For this study, the mean transit time TT was determined by fitting a straight line to the phase difference bins with significant coherence in the HF range (0.2–0.5 Hz), by using a least squares fitting procedure. The mean transit time TT reflects the transit time associated with the relative contributions of both blood flow and blood volume oscillations. Only data sections that yielded at least five consecutive bins with significant coherence were accepted, thereby avoiding inclusion of bins with significant coherence that arose by chance.²⁷ The mean transit time was calculated according to equation (2), and extrapolation of the linear trend outside the HF range was performed by applying equation (1).

Cerebral autoregulation analysis with TT-BF/BV correction

We assume that the measured OxyHb-HHb phase difference is the result of transit time induced phase differences, the relative contribution of blood flow and blood volume oscillations and the effects of cerebral autoregulation. Therefore, to correct the OxyHb-HHb phase difference estimate for transit time effects and blood flow and blood volume oscillations, we subtracted the linear phase trend in the HF range generated by transit time and blood flow and blood volume oscillations from the measured OxyHb-HHb phase difference. After subtraction, the remaining phase difference should then be determined by cerebral autoregulation only.

Statistical analysis

The statistical analysis was performed in SPSS (version 21). Data were expressed as median (IQR) values because of non-normal distributions. Friedman's two-way analysis of variance was used to test for significant differences between the conditions REST vs. DB, REST vs. DBCO₂ and DB vs. DBCO₂, and was applied to the left and right sides, separately. Bonferroni post hoc corrections for multiple comparisons were used in all analyses. Differences between microvascular and macrovascular DCA estimates were evaluated with related samples Wilcoxon signed-rank test. Intraclass correlation (ICC) analysis was used to evaluate the agreement between microvascular and macrovascular TFA results, using the two-way mixed model with absolute agreement option in SPSS. When necessary, data were log-transformed to obtain a normal distribution. ICCs were

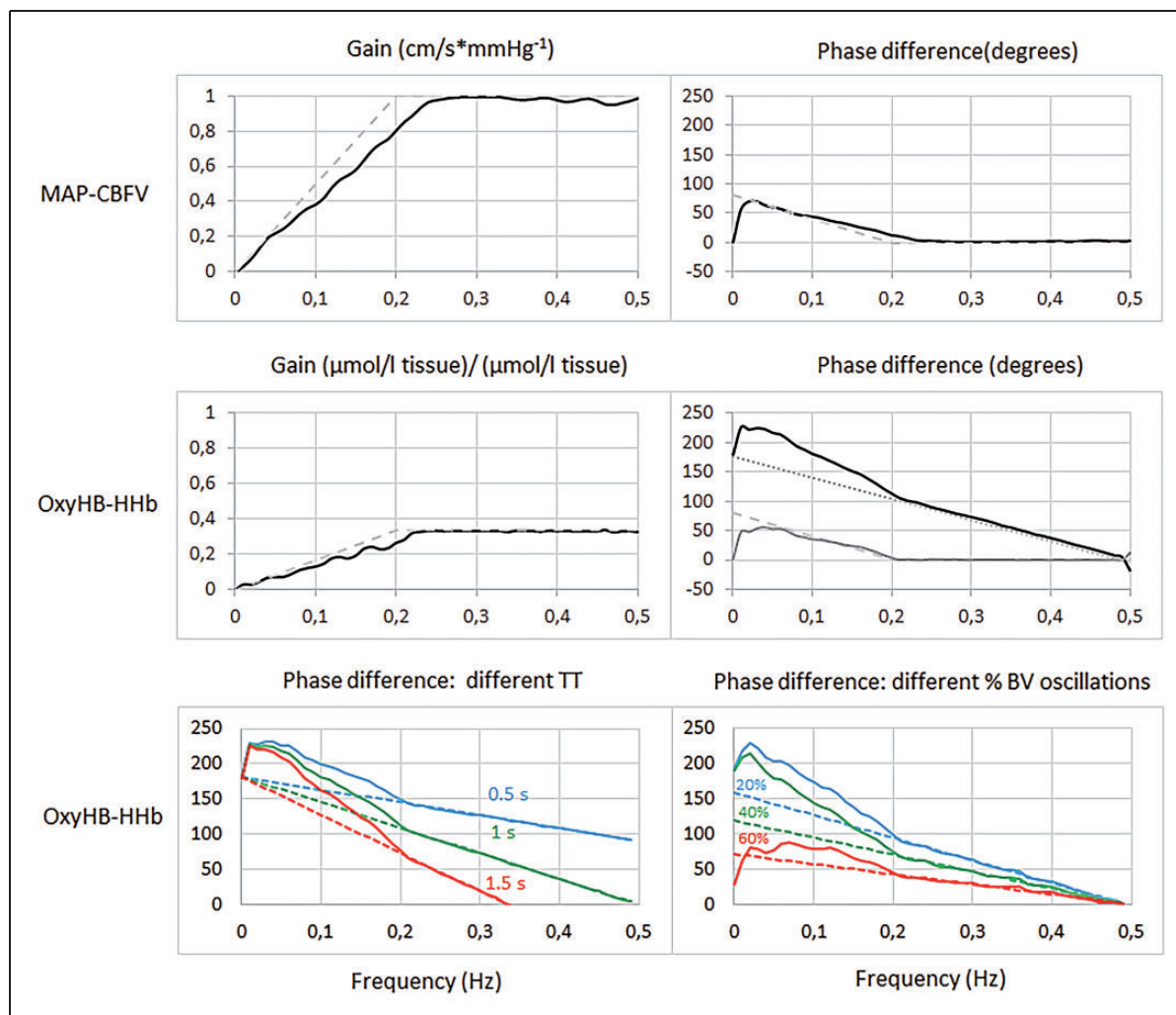


Figure 1. Transfer function results on simulated data. Five data segments were used in the averaging procedure that is part of TFA. Top row: MABP-CBFV comparison: reference data are depicted in grey dashed lines, while solid black lines indicate the TFA results. Middle row: OxyHb-HHb comparison: in the phase difference plot, the dotted line indicates the linear trend in the HF data. Subtracting this linear trend from the OxyHb-HHb data (black solid line) results in the transit time corrected phase difference (solid grey line), which is very close to the reference data. Bottom row: OxyHb-HHb phase difference spectra for different TTs and different percentages of blood volume oscillations (%BV). %BV was varied by changing the percentage of data segments with synchronous OxyHb and HHb oscillations. Note that for different transit times, the Y-axis intercept of the linear phase trend due to transit time does not change but the X-axis intercept does, while for different percentages of blood volume oscillations the X-axis intercept remains constant and the Y-axis intercept changes. For details see Appendix 1, Parts 1 and 2. MABP-CBFV: mean arterial blood pressure-cerebral blood flow velocity; OxyHb-HHb: oxygenated haemoglobin-deoxygenated haemoglobin; TT: transit time; BV: blood volume.

tested for significance by applying an F-test with true value 0. For all tests, we assumed a significance level of $\alpha = 0.05$.

Results

Hemodynamic variables

Table 1 provides an overview of the hemodynamic variables obtained from the 15 participants during the

experiment. MABP increased during DBCO₂ and was significantly higher compared to REST. Heart rate was significantly higher during DB compared to the other conditions, although the absolute difference was only small (± 5 beats/min). ETCO₂ decreased during DB (REST: 5.1 vs. DB: 4.7 kPa, $p = 0.03$). ETCO₂ monitoring was not possible during DBCO₂. As expected, the power in both the LF and VLF range of the ABP signal increased significantly during both DB periods (REST vs. DB vs. DBCO₂: LF: 13.2 vs. 41.1 vs.

Table 1. Hemodynamic variables, MABP-power spectral density data, and statistical comparisons.

Test condition	Median values (IQR)			Post hoc Friedman test (p-value)		
	REST (n = 15)	DB (n = 15)	DBCO ₂ (n = 15)	REST-DB	REST-DBCO ₂	DB-DBCO ₂
MABP (mmHg)	85.1 (20.4)	88.7 (20.7)	95.5 (20.2)	1.0	0.02	0.09
Heart rate (min ⁻¹)	68.1 (22.9)	73.0 (21.3)	68.1 (18.8)	0.03	1.0	0.02
ETCO ₂ (kPa)	5.1(0.6)	4.7 (0.4)	^a	0.03	–	–
MABP PSD (mmHg ² /Hz ⁻¹)						
VLF (0.02–0.07 Hz)	52.8 (65.5)	105.9 (71.3)	110.3 (159.6)	0.02	0.09	1.0
LF (0.07–0.2 Hz)	13.2 (13.2)	41.1 (52.6)	40.5 (44.2)	<0.001	<0.001	1.0
HF (0.2–0.5 Hz)	1.0 (1.1)	1.2 (1.2)	2.2 (2.3)	1.0	0.09	0.09
CBFV (cm/s)						
Left	63.8 (22.0)	48.8 (22.7)	73.6 (30.1)	0.06	0.13	<0.001
Right	60.1 (15.3)	49.5 (15.0)	77.4 (22.6)	0.06	0.13	<0.001
OxyHb (μmol/l tissue)						
Left	0.5 (1.6)	–0.07 (2.2)	2.6 (5.8)	<0.001	<0.001	<0.001
Right	0.5 (0.5)	–0.2 (1.6)	2.7 (6.7)	<0.001	<0.001	<0.001
HHb (μmol/l tissue)						
Left	–0.05 (0.5)	0.1 (0.2)	–2.5 (3.0)	<0.001	<0.001	<0.001
Right	0.0 (0.5)	0.02 (0.9)	–2.4 (2.7)	<0.001	<0.001	<0.001
totalHb (μmol/l tissue)						
Left	0.4 (1.6)	0.08 (1.9)	0.5 (4.6)	<0.001	0.167	<0.001
Right	0.3 (1.6)	–0.3 (1.5)	0.4 (5.1)	<0.001	0.024	<0.001

All values are reported as median (IQR) for the three test conditions: REST, DB and DBCO₂ inhalation; p-values are given for the post hoc Friedman test. The MABP PSD was calculated for the frequency ranges: VLF, LF and HF.

MABP: Mean arterial blood pressure; ETCO₂: end-tidal CO₂; PSD: power spectral density; CBFV: cerebral blood flow velocity; OxyHb: oxyhaemoglobin; HHb: deoxyhaemoglobin; totalHb: total haemoglobin; VLF: very low frequency; LF: low frequency; HF: high frequency; REST: 5-minute periods of rest; DB: deep breathing; DBCO₂: deep breathing with 8% CO₂.

^aEnd-tidal CO₂ monitoring was not possible during the inhalation of 8% CO₂.

40.5 mmHg²·Hz⁻¹, $p < 0.001$ vs. REST for both DB and DBCO₂, VLF: 52.8 vs. 105.9 vs. 110.3 mmHg²·Hz⁻¹, $p = 0.02$ for DB vs. REST, $p = 0.09$ for DBCO₂ vs. REST), but power in the HF range remained unchanged. CBFV decreased during DB, and increased during DBCO₂, with significant differences only between DB and DBCO₂. OxyHb, HHb and totalHb showed highly significant changes between the three conditions, with an increase in OxyHb and totalHb and a decrease in HHb during DBCO₂, and a reversed pattern during DB. Figure 2 shows an example of a raw data recording in a volunteer.

Cerebral autoregulation analysis without TT-BF/BV correction

Tables 2 (LF band data) and 3 (VLF band data) present an overview of the MABP-CBFV and OxyHb-HHb TFA results in the cerebral autoregulation range, without TT-BF/BV correction.

LF band data. Using MABP-CBFV data, a significant phase difference decrease during DBCO₂ (left 23.4°; right 22.9°) was seen compared to DB (left 58.4°; right

54.2°, $p < 0.001$ for both sides) and to a lesser degree also compared to REST (left 35.4°; right 36.1°, left $p = 0.01$, right $p = 0.13$). Relative gain values also decreased significantly during DBCO₂ compared to REST and DB. Coherence increased significantly during DBCO₂ compared to DB, but not compared to REST. Using the OxyHb-HHb data, the phase difference decreased markedly during DBCO₂ compared to REST (left 30.4°; right 57.7°, REST: left 118.2°; right 122.3°, $p < 0.01$ for both sides) but no significant change occurred during DB (left 125.4°; right 139.9°, $p = 1$ for both sides). Gain decreased during DBCO₂, but not significantly for both hemispheres. Coherence showed no clear changes.

VLF band data. Using the MABP-CBFV data, no significant differences between conditions were found for gain or coherence. Although phase values were lower during DBCO₂ and during DB compared to REST, variability was high, and phase was only significantly lower for the left hemisphere for the REST-DBCO₂ comparison. Using the OxyHb-HHb data, no major changes were found for gain or coherence, but phase decreased during DBCO₂, and was significantly different from REST, but not from DB.

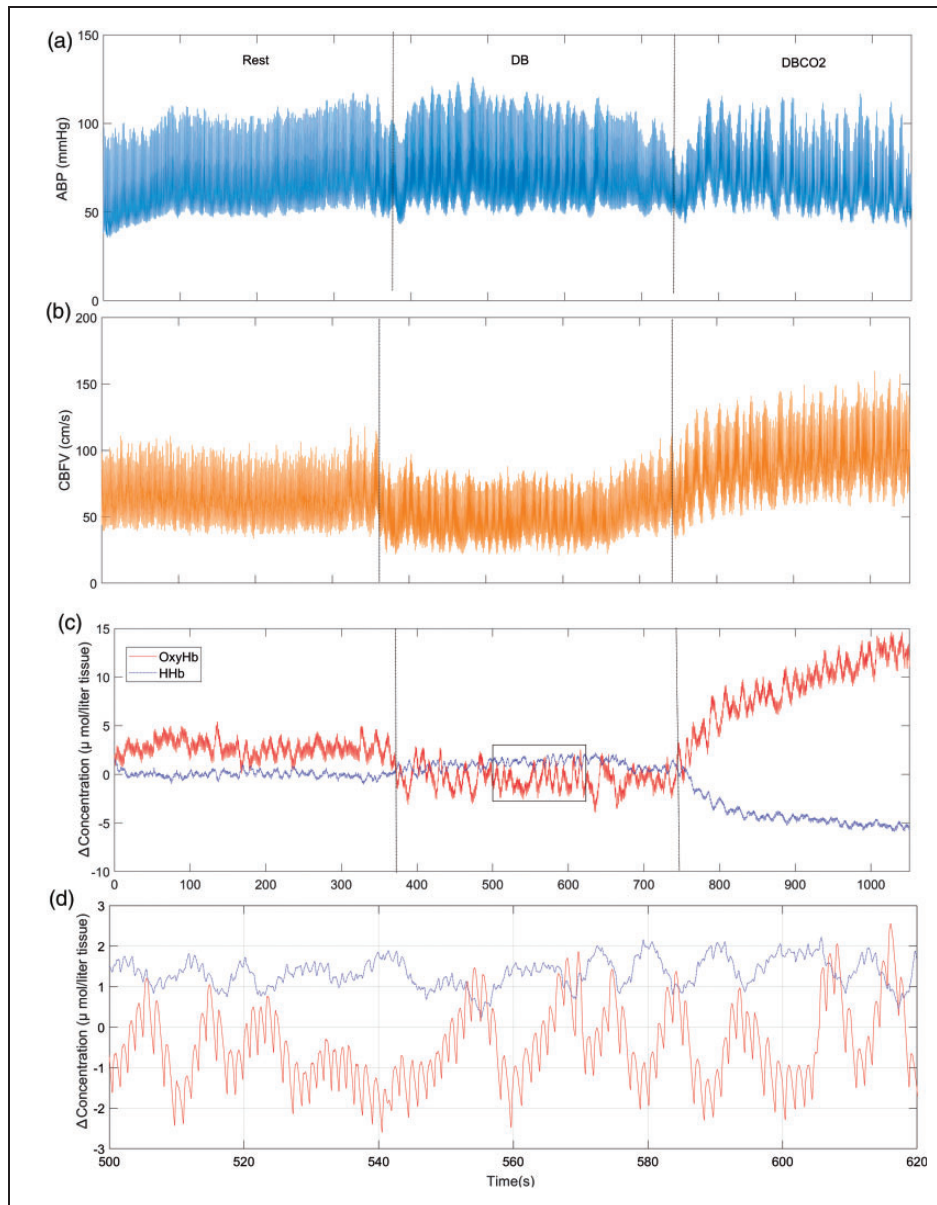


Figure 2. Raw data recording in a representative healthy volunteer: (a) the ABP, (b) the CBFV in the (left) middle cerebral artery and (c) the (left) OxyHb and (left) HHb signals expressed as concentration differences compared to baseline. The vertical lines separate the different conditions. From left to right: REST, DB, and DBCO₂. The lower panel (d) zooms in on the 120 s of data during the DB task framed in (c), which shows the typical antiphase relation between OxyHb and HHb for slow oscillations during high blood flow conditions. Note that the amplitude of oscillations in the OxyHb signal was higher compared to the HHb signal, with increasing amplitudes during both DB periods. During DBCO₂, CBFV and OxyHb increase clearly with a comparatively smaller decrease in absolute values of HHb, which is caused by increased CBF and CBV during hypercapnia while assuming stable brain metabolism. ABP: arterial blood pressure; CBFV: cerebral blood flow velocity; OxyHb: oxygenated haemoglobin; HHb: deoxygenated haemoglobin.

OxyHb-HHb vs. *MABP-CBFV*. When comparing the OxyHb-HHb analysis with the MABP-CBFV analysis, gain was much lower for OxyHb-HHb in all conditions for both the VLF and LF band (all comparisons $p < 0.05$). The phase difference was consistently and significantly higher for the OxyHb-HHb analysis in all conditions and for both the VLF and LF band data (all comparisons $p < 0.05$), but the median

(OxyHb-HHb) – (MABP-CBFV) phase difference was much smaller during DBCO₂ (VLF: left 75.0° right 66.9°, LF: left 40.8° right 17.8°) compared to REST (VLF: left 117.5° right 110.2°, $p > 0.05$ for both sides, LF: left 85.7° right 83.9°, left $p < 0.001$ right $p = 0.004$) and DB (VLF: left 140.8° right 130.9°, $p > 0.05$ for both sides, LF: left 82.7° right 69.6°, left $p = 0.032$ right $p = 0.017$), although these

Table 2. Transfer function analyses and statistical comparisons: LF band data.

Test condition	Side	Median values (IQR)			Post hoc Friedman test (p-value)		
		REST (n = 15)	DB (n = 15)	DBCO ₂ (n = 15)	REST-DB	REST-DBCO ₂	DB-DBCO ₂
MABP-CBFV							
Gain (cm/s)/mmHg	Left	1.0 (0.5)	0.9 (0.5)	0.9 (0.5)	NC	NC	NC
	Right	1.1 (0.6)	0.8 (0.4)	0.8 (0.4)	0.006	0.002	1.0
Gain (%/%)	Left	1.5 (0.3)	1.6 (0.7)	1.1 (0.3)	0.82	0.02	<0.001
	Right	1.5 (0.5)	1.4 (0.2)	1.1 (0.3)	1.0	0.001	0.002
Phase (°)	Left	35.4 (17.6)	58.4 (30.7)	23.4 (18.2)	0.01	0.20	<0.001
	Right	36.1 (10.1)	54.2 (24.7)	22.9 (24.7)	0.13	0.03	<0.001
Coherence	Left	0.7 (0.2)	0.6 (0.1)	0.8 (0.2)	0.30	0.30	0.003
	Right	0.7 (0.2)	0.6 (0.2)	0.8 (0.2)	0.13	0.43	0.002
OxyHb-HHb							
Gain (µmol/l tissue)/ (µmol/l tissue)	Left	0.2 (0.1)	0.3 (0.1)	0.2 (0.1)	1.0	0.09	0.02
	Right	0.3 (0.1)	0.3 (0.1)	0.2 (0.1)	1.0	0.04	0.11
Gain (%/%)	Left	0.5 (0.2)	0.5 (0.3)	0.3 (0.1)	1.0	0.03	0.01
	Right	0.5 (0.3)	0.5 (0.3)	0.3 (0.2)	1.0	0.05	0.13
Phase (°)	Left	118.2 (52.4)	125.4 (49.3)	30.4 (59.1)	1.0	<0.001	0.02
	Right	122.3 (41.7)	139.9 (56.5)	57.7 (72.8)	1.0	0.007	0.004
Coherence	Left	0.5 (0.2)	0.4 (0.2)	0.6 (0.3)	1.0	0.20	0.03
	Right	0.4 (0.3)	0.5 (0.3)	0.5 (0.2)	NC	NC	NC

Transfer function analysis with input parameters MABP and OxyHb and output parameters CBFV in the middle cerebral artery and HHb, respectively. Values are given as median values (IQR) for the three test conditions; REST, DB and DBCO₂; p-values are given for the post hoc Friedman test. NC indicates no post-hoc statistics were calculated as the Friedman test detected no overall significance difference. Gain (%/%) refers to normalised data while (cm/s)/mmHg and (µmol/l tissue)/(µmol/l tissue) refer to data that were mean subtracted. Coherence: values are means of the LF band. MABP: Mean arterial blood pressure; CBFV: cerebral blood flow velocity; OxyHb: oxyhaemoglobin; HHb: deoxyhaemoglobin; totalHb: total haemoglobin; LF: low frequency; REST: 5-minute periods of rest; DB: deep breathing; DBCO₂: deep breathing with 8% CO₂.

differences were only significant for the LF band data. The ICC analysis showed a uniform absence of significant agreement between OxyHb-HHb and MABP-CBFV TFA results, for both gain and phase in both the VLF and LF band during all conditions. Regression analysis also showed an absence of a significant linear relation between uncorrected OxyHb-HHb and MABP-CBFV phase differences during all conditions, except for the right sided measurements during DBCO₂ (MABP-CBFV = 13.7 + 0.14 × OxyHb-HHb phase difference, p = 0.01). Coherence was lower in all conditions for OxyHb-HHb compared to MABP-CBFV for the LF band data but not for the VLF band data.

Cerebral autoregulation analysis with TT-BF/BV correction

Figure 3 shows the grand average phase difference spectra for all three conditions and is based on the data of all 15 subjects. During REST and DB, subtraction of the linear trend in the HF data results in a phase difference spectrum that is very similar to the MABP-CBFV phase difference spectrum. This result is qualitatively equal to the result that was obtained using the

simulated data (Figure 1). However, during DBCO₂, the slope of the linear trend in the HF data is almost zero, suggesting a high percentage of blood volume changes, and subtraction of this trend does not result in major changes in the OxyHb-HHb spectrum. Note that despite the different slopes, the X-axis intercept for the linear phase difference trend is similar for all three conditions. For the LF band, the OxyHb-HHb and MABP-CBFV phase difference spectra are still similar, but for the VLF the difference is high. This result was not predicted from analysis of the simulated data.

Table 4 shows the results of the cerebral autoregulation analysis after TT-BF/BV correction in individual subjects. In four subjects, coherence in the HF band was insufficient for reliable calculation of transit time. These subjects were left out of the analysis which is presented in Table 4.

During all conditions, median phase differences were not significantly different between MABP-CBFV and corrected OxyHb-HHb, except for the VLF band data on the left side during DBCO₂, which showed higher values for corrected OxyHb-HHb compared to MABP-CBFV (52.3° vs. 30.3°, p = 0.03). All (MABP-CBFV) – (corrected OxyHb-HHb) phase differences

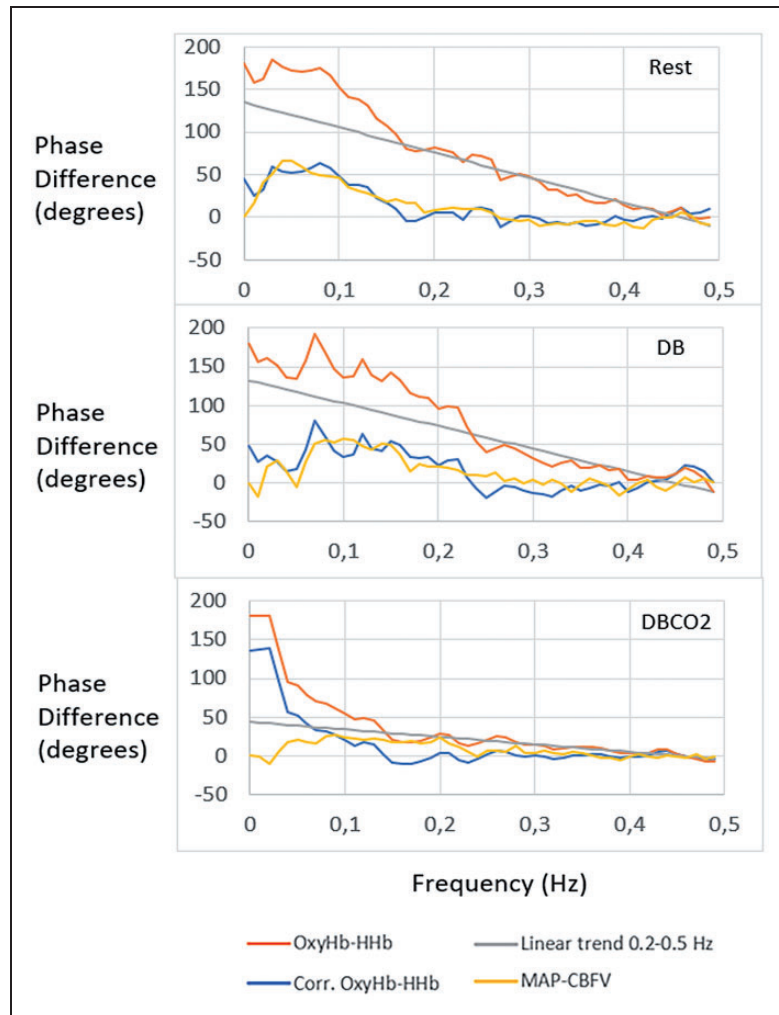


Figure 3. Grand average phase difference spectrum results. The grand average mean arterial blood pressure (MABP)-cerebral blood flow velocity (CBFV) phase difference and oxyhaemoglobin (OxyHb)- deoxyhaemoglobin (HHb) phase difference for the frequency range 0–0.5 Hz for REST, DB and DBCO₂. Outside the autoregulatory frequency range in the HF band, the MABP-CBFV phase shift (yellow lines) fluctuates around 0° for the three conditions, indicating that these calculations are not influenced by transit time. This is the typical spectral profile of a parallel system. The OxyHb-HHb HF phase difference shows a linear trend during REST and DB (grey lines). This is the typical spectral profile of a serial system with transit time. Subtracting the linear trend from the OxyHb-HHb phase difference results in the TT-BF/BV corrected OxyHb-HHb phase difference (blue lines). Note that during REST and DB, the TT-BF/BV corrected phase difference is very similar to the MABP-CBFV phase difference. During CO₂ inhalation (DBCO₂), the slope of the linear phase difference trend decreases, indicating a decrease in mean transit time. However, the X-axis intercept does not change compared to REST and DB, suggesting prominent blood volume changes. In the VLF range, blood flow changes remain dominant, and a mismatch between the MABP-CBFV and TT-BF/BV corrected OxyHb-HHb phase difference spectrum is present. MABP-CBFV: mean arterial blood pressure-cerebral blood flow velocity; OxyHb-HHb: oxygenated haemoglobin-deoxygenated haemoglobin; DBCO₂: deep breathing with the inhalation of 8% CO₂.

were much lower compared to the autoregulation analysis without TT-BF/BV correction. The ICC analysis indicated significant agreement between MABP-CBFV and corrected OxyHb-HHb phase differences for the LF band data during rest and DB on both sides, but for the VLF band and HF band no significant agreement was found. The mean absolute phase difference between MABP-CBFV and corrected OxyHb-HHb was

much lower for the LF and HF band data compared to the VLF band data.

The mean transit time was similar during REST (left 0.68 ± 0.23 , right 0.74 ± 0.20) and DB (left 0.70 ± 0.63 , right 0.87 ± 0.34), but decreased markedly during DBCO₂ (left: 0.22 ± 0.32 , right 0.33 ± 0.13 , $p < 0.05$ vs. REST and DB for both sides). However, the transit time related to blood flow changes was remarkably

Table 3. Transfer function analyses and statistical comparisons: VLF band data.

Test condition	Side	Median values (IQR)			Post hoc Friedman test (p-value)		
		REST (n = 15)	DB (n = 15)	DBCO ₂ (n = 15)	REST-DB	REST-DBCO ₂	DB-DBCO ₂
MABP-CBFV							
Gain (cm/s)/mmHg	Left	0.5 (0.5)	0.6 (0.4)	0.6 (0.2)	NC	NC	NC
	Right	0.7 (0.4)	0.6 (0.4)	0.6 (0.3)	NC	NC	NC
Gain (%/%)	Left	0.8 (0.3)	0.9(0.5)	0.8 (0.3)	NC	NC	NC
	Right	0.9 (0.3)	1.0 (0.6)	0.8 (0.3)	NC	NC	NC
Phase (°)	Left	52.0 (47.2)	36.6 (36.3)	26.3 (28.9)	0.15	0.02	1.0
	Right	54.4 (18.1)	24.5 (38.1)	25.9 (29.3)	0.12	0.07	1.0
Coherence	Left	0.3 (0.2)	0.4 (0.2)	0.5 (0.2)	NC	NC	NC
	Right	0.3 (0.3)	0.4 (0.2)	0.5 (0.3)	0.6	0.06	0.20
OxyHb-HHb							
Gain (µmol/l tissue)/ (µmol/l tissue)	Left	0.3 (0.1)	0.2 (0.2)	0.2 (0.1)	0.79	0.01	0.22
	Right	0.3 (0.2)	0.3 (0.1)	0.2 (0.1)	NC	NC	NC
Gain (%/%)	Left	0.6 (0.1)	0.5 (0.2)	0.4 (0.2)	0.20	0.03	1.0
	Right	0.6 (0.2)	0.5 (0.1)	0.3 (0.1)	0.43	0.01	0.43
Phase (°)	Left	166.6 (53.5)	161.9 (91.4)	80.0 (91.3)	0.22	0.01	0.79
	Right	172.1 (18.1)	165.0 (45.8)	117.1 (85.1)	0.35	0.005	0.35
Coherence	Left	0.4 (0.4)	0.3 (0.4)	0.4 (0.4)	NC	NC	NC
	Right	0.5 (0.3)	0.4 (0.3)	0.4 (0.2)	NC	NC	NC

Transfer function analysis with input parameters MABP and OxyHb and output parameters CBFV in the middle cerebral artery) and HHb, respectively. Values are given as median values (IQR) for the three test conditions; REST, DB and DBCO₂; p-values are given for the post hoc Friedman test. NC indicates no post-hoc statistics were calculated as Friedman test detected no overall significance difference. Gain (%/%) refers to normalised data while (cm/s)/mmHg and (µmol/l tissue)/(µmol/l tissue) refer to data that were mean subtracted. Coherence: values are means of the VLF band. MABP: Mean arterial blood pressure; CBFV: cerebral blood flow velocity; OxyHb: oxyhaemoglobin; HHb: deoxyhaemoglobin; totalHb: total haemoglobin; VLF: very low frequency; REST: 5-minute periods of rest; DB: deep breathing; DBCO₂: deep breathing with 8% CO₂.

stable during all conditions, with mean values of around 1.1 to 1.2s, with no significant differences between the three conditions. The estimated percentage of blood flow changes was similar during REST (left 66 ± 22 , right 73 ± 16) and DB (left 63 ± 28 , right 65 ± 23), but decreased significantly during DBCO₂ (left 21 ± 31 , right 26 ± 19 , $p < 0.05$ vs. REST and DB for both sides).

Discussion

In this study, we performed detailed analysis of MABP, CBFV and NIRS signals to answer the question if microvascular- and macrovascular-based estimates of DCA are similar. The comparisons were made both with and without TT-BF/BV correction. TT-BF/BV correction was implemented by applying the constant time lag plus constant phase shift model, which is a well-known model for the analysis of serial systems in the frequency domain. Our main findings are:

1. Without TT-BF/BV correction, microvascular-based estimates of cerebral autoregulation are different

from macrovascular-based estimates of cerebral autoregulation, with much higher phase differences for microvascular-based estimates in all conditions.

2. Transit time and the percentage of blood flow and blood volume oscillations can be calculated from the OxyHb-HHb phase difference spectrum in the HF band by using the constant time lag plus constant phase shift model, provided that coherence is large enough for reliable analysis.
3. After TT-BF/BV correction, microvascular-based estimates of DCA are similar to macrovascular-based DCA estimates. For grand average data, this is true for the entire phase difference spectrum, while for individual data this applies to the LF band only.
4. DBCO₂ resulted in a decrease of both microvascular and macrovascular measurement-based phase differences in the LF band, but not in the VLF band. A decrease in mean transit time was also observed, but the transit time related to blood flow oscillations was remarkably stable during all conditions. During DBCO₂, the percentage of blood volume oscillations increased in the LF and HF band, but not in the VLF band.

Table 4. Results of the phase difference values between OxyHb and HHb after TT-BF/BV correction.

Frequency Band	Corrected OxyHb-HHb	MABP-CBFV	p-value	Mean Abs Error	ICC	TT mean	TT BF	%BF
REST								
VLF left	48.7 (23.4)	46.3 (11.5)	>0.05	17.2 (27.4)	-0.14			
VLF right	46.1 (34.5)	40.9 (12.3)	>0.05	33.6 (67.8)	0.1			
LF left	30.7 (7.5)	29.5 (6.5)	>0.05	4.5 (7.2)	0.60 ^a			
LF right	39.6 (23.6)	32.6 (8.9)	>0.05	9.8 (9.5)	0.56 ^a			
HF left	4.1 (5.6)	1.2 (6.3)	>0.05	4.3 (3.3)	-0.07	0.68 (0.23)	1.14 (0.14)	66 (22)
HF right	6.8 (6.8)	0.2 (7.8)	>0.05	6.0 (10.0)	-0.36	0.74 (0.20)	1.14 (0.10)	73 (16)
DB								
VLF left	59.5 (50.9)	27.1 (7.7)	>0.05	35.6 (38.6)	0.44			
VLF right	66.7 (75.0)	29.7 (4.6)	>0.05	60.9 (22.5)	-0.62			
LF left	43.3 (29.4)	48.6 (20.9)	>0.05	10.6 (11.7)	0.73 ^a			
LF right	61.8 (32.6)	52.1 (10.9)	>0.05	8.5 (17.3)	0.70 ^a			
HF left	1.1 (19.7)	1.9 (11.3)	>0.05	9.5 (12.8)	-0.03	0.70 (0.63)	1.22 (0.20)	63 (28)
HF right	7.3 (4.9)	5.8 (7.8)	>0.05	10.0 (8.3)	0.17	0.87 (0.34)	1.14 (0.22)	65 (23)
DBCO₂								
VLF left	52.3 (72.3)	30.3 (16.1)	0.03	53.9 (31.3)	0.42			
VLF right	65.6 (57.0)	23.4 (17.9)	>0.05	51.1 (31.9)	-0.21			
LF left	27.9 (22.2)	20.4 (9.0)	>0.05	14.0 (6.5)	0.33			
LF right	19.8 (14.7)	21.2 (11.8)	>0.05	8.8 (7.0)	0.37			
HF left	2.2 (5.0)	3.5 (6.3)	>0.05	6.1 (10.4)	-0.17	0.22 (0.32) ^b	1.11 (0.22)	21 (31) ^b
HF right	5.4 (5.2)	4.0 (11.4)	>0.05	9.9 (4.2)	-0.28	0.33 (0.13) ^b	1.22 (0.18)	26 (19) ^b

Due to lack of sufficient coherence in the HF band, 4 subjects were left out of the analysis, leaving 11 subjects for this analysis. For comparison, the MABP-CBFV phase difference is also presented. Mean Abs error: mean of the absolute angular difference between the corrected OxyHb-HHb and MABP-CBFV phase difference; ICC: intraclass correlation coefficient; TT mean: mean transit time; TT BF: transit time for blood flow changes; %BF: estimated percentage of blood flow changes.

^aICC value significantly different from 0.

^bSignificant difference vs. REST and DB for TT mean and %BF.

Cerebral autoregulation estimates without TT-BF/BV correction

The finding that macrovascular- and microvascular-based estimates of DCA are different was expected and can be explained by the transit time effects and blood flow and blood volume effects that are present for the microvascular-based estimates and absent for macrovascular-based estimates. In response to DB and DBCO₂, LF phase differences between MABP and CBFV increased and decreased, respectively. This is a well-known phenomenon and has been reported several times by other authors and was interpreted as a stronger vs. weaker autoregulatory response during hypo- and hypercapnia respectively.^{19,31,32} The uncorrected OxyHb-HHb VLF and LF phase differences showed a similar pattern, but the values were significantly higher compared to the MABP-CBFV phase difference during all conditions. With DBCO₂, this difference was significantly lower compared to the other conditions. This can be explained by the increase in cerebral blood volume oscillations during hypercapnia which will decrease the

mean transit time due to the 0-s transit time that is associated with blood volume oscillations. The lack of any agreement and the prevailing lack of a significant linear relation between uncorrected microvascular- and macrovascular-based cerebral autoregulation estimates demonstrate that uncorrected OxyHb-HHb phase differences cannot be used to estimate cerebral autoregulation.

Transit time, blood flow and blood volume oscillations

The results of the OxyHb-HHb grand average data during rest and DB are very similar to the simulated data results, which strongly suggest that the underlying assumptions behind the constant time lag plus constant phase shift model are correct during these conditions. However, during DBCO₂, the VLF band results deviated from what was predicted by the simulated data, probably because the assumption that blood volume oscillations would increase for every frequency is not correct. The brain is encased in a rigid skull, which may not allow unlimited blood volume changes.^{15,33} Especially for the VLF band, induced

oscillations are of high amplitude, which may exceed the limits of blood volume expansion induced by hypercapnia. Therefore, blood flow changes must occur in order to prevent a rise in intracranial pressure. For higher frequencies, blood volume changes are of lower amplitude and blood volume changes may not be limited during hypercapnia.

On individual data, in 4 out of 15 subjects, coherence was too small for reliable calculations of transit time and percentages of blood flow and blood volume oscillations. This was probably caused by noise, or by insufficient power in the HF band, in combination with measurements of relatively short duration. The confidence limits of the phase difference spectra depend on the size of coherence and the number of data segments used in the averaging procedure for TFA.^{34,35} Using data with low coherence will increase the confidence limits and will therefore result in major error when calculating transit time and blood flow and blood volume oscillations. The solution to this problem could either be to use manoeuvres to increase coherence in the HF band or to increase the duration of the measurement to increase the number of data segments that are used for averaging during TFA. When comparing our transit times with those reported in other types of studies, the average microvascular transit times are quite similar for both human⁵ and animal^{36,37} data, which supports the validity of these measurements.

Cerebral autoregulation estimates with TT-BF/BV correction

For individual data, after correcting the OxyHb-HHb phase difference spectrum using the constant time lag plus constant phase difference model, the mean absolute difference with the MABP-CBFV phase spectrum was low for the LF band and HF band, but high for the VLF band data. A significant agreement between OxyHb-HHb and MABP-CBFV phase differences was found for the LF band data during REST and DB, but not during DBCO₂. With similar mean absolute phase differences between OxyHb-HHb and MABP-CBFV in the LF band during the three conditions, this can be explained by a reduced range of phase difference values during DBCO₂, which will reduce any correlation-based indices including ICC. Therefore, the lower ICC values in the LF band during DBCO₂ do not indicate an increase in error or a true decrease in agreement. A similar explanation can account for a lack of agreement in the HF band data. For the VLF band, coherence values were on average much lower compared to the LF band data (0.3 vs. 0.7, Tables 2 and 3) for MABP-CBFV, but not for OxyHb-HHb. This will increase the error in the phase estimates for MABP-CBFV and will cause a reduced agreement

with the OxyHb-HHb estimates. From these results, we can conclude that the LF band data can provide the most reliable estimates of cerebral autoregulation. In the VLF band, the autoregulation system may exhibit strong non-linear and non-stationary properties, or there may be contribution of other variables that cannot be measured.^{38,39} Although there may be valuable information in the VLF band, the TFA that was used in the present study does not produce reliable estimates of cerebral autoregulation in this frequency band.

Contrary to other studies,⁵ we found a significant agreement between microvascular and macrovascular phase difference estimates of cerebral autoregulation in the LF band, which is to the best of our knowledge a unique finding which has never been reported in the literature. Other studies that have directly compared microvascular with macrovascular estimates of DCA have reported correlations with MABP and NIRS variables only^{11,40} and did not evaluate agreement (i.e. ICC analysis) but reported associations or correlations.⁹ However, recently DCA estimates obtained with the technique of diffuse correlation spectroscopy DCS showed good agreement with regulation rates measured by TCD.¹⁰ Although time domain DCA estimates based on thigh cuff induced blood pressure decreases were used in that study, the finding of good agreement between microvascular- and macrovascular-based estimates of DCA is essentially similar to the results presented in our study. The fact that high levels of agreement between microvascular- and macrovascular-based estimates of DCA can be found with different techniques and with both time domain and frequency domain estimates of DCA further supports the interpretation that microvascular- and macrovascular-based estimates of DCA can be used to measure the same physiological process. When comparing our method with the DCS method, the advantage of our method is that it can be applied to spontaneous blood pressure oscillations without the need for using thigh cuffs. Another advantage is that blood pressure measurement is not necessary for the determination of microvascular DCA in our method, while for the rate of regulation parameter in the DCS method, a continuous blood pressure measurement is required. Because measurement of DCA based on NIRS variables alone has practical benefit, we focused on the OxyHb-HHb comparison in this study. However, it is possible to use the same analysis strategy on different variable combinations (MABP vs. NIRS, CBFV vs. NIRS), and such extensions of this methodology can be further explored in the future.

The effects of hypercapnia

During REST and DB, the results of the analysis with the constant time lag plus constant phase difference

model suggest dominant blood flow oscillations, with a minor contribution of blood volume changes. During DBCO₂, we found very high levels of blood volume changes in the LF and HF band, which was accompanied by a decrease in mean transit time compared to REST and DB. However, the transit time associated with blood flow changes showed very little change, which suggests that the primary change induced by different levels of CO₂ is the percentage of cerebral blood volume changes, and not a change of the capillary transit time itself. Highly similar results were found in the simulation study, which further supports this interpretation. Similar findings have been published recently, where hypocapnia due to hyperventilation did not result in an altered transit time estimate, but blood volume estimates changed.⁵

The finding of an unchanged transit time associated with blood flow changes during very different conditions with a different balance between oscillations in cerebral blood flow and blood volume is hard to explain using a simple serial capillary system model. We speculate that during hypercapnia, parallel vascular channels such as metarterioles could be recruited and may act as capacitance vessels and arteriovenous shunt channels. The system would then change to a parallel system, with constant transit time in the capillary part, while in the metarterioles oscillations in OxyHb could synchronise with capillary venous oscillations in HHb, to result in a transit time near 0 s. This theory is further explained and illustrated in Appendix 1, Part 3.

Limitations

Firstly, this is a relatively small study with relatively short recordings, and although the main effects are clear, the findings should be expanded to a larger cohort. The sex ratio was heavily skewed towards females in our study population, and it is known that females have different DCA status compared to males.⁴¹ However, the main results of this study should not be affected by the skewed sex distribution, as the most important results are based on intraindividual differences between techniques and conditions.

Secondly, we used DBCO₂ in this experiment, but we were unable to measure to which degree the CO₂ level was changed by 8% CO₂ inhalation. Therefore, we were unable to verify if the level of hypercapnia was related to the change in autoregulation, mean transit time and cerebral blood volume oscillation estimates. Similarly, hypocapnia was not controlled in this experiment. We prioritised the measurement protocol towards random breathing instructions, rather than attaining a fixed level of hypocapnia, because establishing blood pressure oscillations is essential for estimating cerebral autoregulation. It is also possible that DB

and DBCO₂ induced changes in cerebral venous pressure or ICP, but we were not able to verify if such changes occurred and therefore were not able to correct for them. This may have contributed to variability of the measurements and analysis.

Thirdly, the constant time lag plus constant phase shift model was not applicable in every subject due to low coherence. This limits application in individual subjects or patients. Future studies should find ways to increase applicability in every subject or patient. A logical first approach would be to find ways to increase coherence, for example by employing other methods to induce blood pressure oscillations or by using longer registration periods. Compared to other microvascular models,⁶ the constant time lag plus constant phase shift model is relatively simple and does not consider other factors such as arterial oxygen saturation, capillary lengths and diffusion coefficients. However, even with a relatively simple model, we observe a significant agreement between MABP-CBFV and OxyHb-HHb oscillations and between simulated data and physiological data, which suggests that the underlying assumptions are realistic. This does not mean that there is no room for improvement; it could be that agreement would increase when other factors are accounted for. On the other hand, one has to aim for the minimum number of variables needed to adequately describe the data and be critical towards the added value of any new variable that is introduced.

Fourth, NIRS measurements are not spatially resolved and although we used a 40 mm optode distance, we cannot exclude contributions from extracranial tissue. However, the finding of similarity between MABP-CBFV and corrected OxyHb-HHb phase differences strongly suggest that at least the oscillatory components of the NIRS signals were predominantly determined by brain tissue. Furthermore, the OxyHb-HHb phase difference spectrum during REST and DB was compatible with dominance of blood flow oscillations, which is typical for brain tissue and atypical for extracranial tissue.²⁸ NIRS is also a focal measurement and since we only measured in the MCA territory, we cannot generalise our findings to other vascular territories, which precludes investigation of regional heterogeneity of cerebral autoregulation. Finally, the reproducibility of the findings has not yet been established, and longer measurements may be needed to evaluate if the NIRS-based autoregulation estimates and transit time and blood flow/volume estimates are stable over time and react similarly to repeated challenges.

To conclude, NIRS can provide estimates of DCA that are similar to TCD-based DCA estimates. This is achieved by correcting for transit time and the balance between blood flow and blood volume oscillations,

which can be estimated from the OxyHb-HHb phase difference spectrum in the HF band. The transit time and the balance between blood flow and blood volume oscillations may also provide additional valuable information about cerebral microvascular function. These findings may increase the feasibility of non-invasive continuous autoregulation monitoring and guided therapy in clinical situations.

Funding

The author(s) received no financial support for the research, authorship, and/or publication of this article.

Acknowledgements

The authors wish to thank Miranda Schenk for assistance during the measurements and Lucas Dijck for technical assistance. The authors wish to thank Bauke de Jong for his suggestions and critically reading the manuscript.

Declaration of conflicting interests

The author(s) declared no potential conflicts of interest with respect to the research, authorship, and/or publication of this article.

Authors' contributions

JWJE and JT designed the study, performed experiments, collected and analysed data and wrote the manuscript. MJHA designed the study and contributed to interpretation of data. MC and NMM contributed to interpretation of data. All authors critically reviewed the manuscript and approved the final version to be published.

Supplementary material

Supplementary material for this paper can be found at the journal website: <http://journals.sagepub.com/home/jcb>

References

1. Claassen JA, Meel-van den Abeelen AS, Simpson DM, et al. Transfer function analysis of dynamic cerebral autoregulation: a white paper from the International Cerebral Autoregulation Research Network. *J Cereb Blood Flow Metab* 2016; 36: 665–680.
2. Panerai RB. Transcranial Doppler for evaluation of cerebral autoregulation. *Clin Auton Res* 2009; 19: 197–211.
3. Zhang R, Zuckerman JH, Giller CA, et al. Transfer function analysis of dynamic cerebral autoregulation in humans. *Am J Physiol Hear Circ Physiol* 1998; 274: H233–H241.
4. Pierro ML, Kainerstorfer JM, Civileto A, et al. Reduced speed of microvascular blood flow in hemodialysis patients versus healthy controls: a coherent hemodynamics spectroscopy study. *J Biomed Opt* 2014; 19: 26005.
5. Kainerstorfer JM, Sassaroli A, Tgavalekos KT, et al. Cerebral autoregulation in the microvasculature measured with near-infrared spectroscopy. *J Cereb Blood Flow Metab* 2015; 35: 959–966.
6. Fantini S. Dynamic model for the tissue concentration and oxygen saturation of hemoglobin in relation to blood volume, flow velocity, and oxygen consumption: implications for functional neuroimaging and coherent hemodynamics spectroscopy (CHS). *Neuroimage* 2014; 85: 202–221.
7. Huppert TJ, Allen MS, Diamond SG, et al. NIH public access. Estimating cerebral oxygen metabolism from fMRI with a dynamic multi-compartment windkessel model. *Hum Brain Mapp* 2009; 30: 1548–1567.
8. Brady KM, Lee JK, Kibler KK, et al. Continuous time-domain analysis of cerebrovascular autoregulation using near-infrared spectroscopy. *Stroke* 2007; 38: 2818–2825.
9. Reinhard M, Wehrle-Wieland E, Grabiak D, et al. Oscillatory cerebral hemodynamics—the macro- vs. microvascular level. *J Neurol Sci* 2006; 250: 103–109.
10. Parthasarathy AB, Gannon KP, Baker WB, et al. Dynamic autoregulation of cerebral blood flow measured non-invasively with fast diffuse correlation spectroscopy. *J Cereb Blood Flow Metab* 2018; 38: 230–240.
11. Müller MW-D, Österreich M, Müller A, et al. Assessment of the brain's macro- and micro-circulatory blood flow responses to CO₂ via transfer function analysis. *Front Physiol* 2016; 7: 162.
12. Moerman A and De Hert S. Recent advances in cerebral oximetry. Assessment of cerebral autoregulation with near-infrared spectroscopy: myth or reality? *F1000Res* 2017; 6: 1615.
13. Blauert J and Laws P. Group delay distortions in electroacoustical systems. *J Acoust Soc Am* 1978; 63: 1478–1483.
14. Wolf M, Wolf U, Toronov V, et al. Different time evolution of oxyhemoglobin and deoxyhemoglobin concentration changes in the visual and motor cortices during functional stimulation: a near-infrared spectroscopy study. *Neuroimage* 2002; 16: 704–712.
15. Kainerstorfer JM, Sassaroli A and Fantini S. Optical oximetry of volume-oscillating vascular compartments: contributions from oscillatory blood flow. *J Biomed Opt* 2016; 21: 101408.
16. Grosse P, Guerrini R, Parmeggiani L, et al. Abnormal corticomuscular and intermuscular coupling in high-frequency rhythmic myoclonus. *Brain* 2003; 126: 326–342.
17. Mima T and Hallett M. Corticomuscular coherence: a review. *J Clin Neurophysiol* 1999; 16: 501–511.
18. Ainslie PN, Celi L, McGrattan K, et al. Dynamic cerebral autoregulation and baroreflex sensitivity during modest and severe step changes in arterial PCO₂. *Brain Res* 2008; 1230: 115–124.
19. Panerai R, Deverson S, Mahony P, et al. Effect of CO₂ on dynamic cerebral autoregulation measurement. *Physiol Meas* 1999; 20: 265.
20. Gutiérrez-Jiménez E, Angleys H, Rasmussen PM, et al. The effects of hypercapnia on cortical capillary transit time heterogeneity (CTH) in anesthetized mice. *J Cereb Blood Flow Metab* 2018; 38: 290–303.
21. Ito H, Ibaraki M, Kanno I, et al. Changes in the arterial fraction of human cerebral blood volume during hypercapnia and hypocapnia measured by positron emission tomography. *J Cereb Blood Flow Metab* 2005; 25: 852–857.

22. Reinhard M, Müller T, Guschlbauer B, et al. Transfer function analysis for clinical evaluation of dynamic cerebral autoregulation – a comparison between spontaneous and respiratory-induced oscillations. *Physiol Meas* 2003; 24: 27–43.
23. Claassen JAHR, Levine BD and Zhang R. Dynamic cerebral autoregulation during repeated squat-stand maneuvers. *J Appl Physiol* 2009; 106: 153–160.
24. Birch AA, Dirnhuber MJ, Hartley-Davies R, et al. Assessment of autoregulation by means of periodic changes in blood pressure. *Stroke* 1995; 26: 834–837.
25. Elting JW, Aries MJH, van der Hoeven JH, et al. Reproducibility and variability of dynamic cerebral autoregulation during passive cyclic leg raising. *Med Eng Phys* 2014; 36: 585–591.
26. Berens P. CircStat: a MATLAB toolbox for circular statistics. *J Stat Softw* 2009; 31: 1–21.
27. Mima T, Steger J, Schulman AE, et al. Electroencephalographic measurement of motor cortex control of muscle activity in humans. *Clin Neurophysiol* 2000; 111: 326–337.
28. Tgavalekos KT, Kainerstorfer JM, Sassaroli A, et al. Blood-pressure-induced oscillations of deoxy- and oxy-hemoglobin concentrations are in-phase in the healthy breast and out-of-phase in the healthy brain. *J Biomed Opt* 2016; 21: 101410.
29. Obrig H, Neufang M, Wenzel R, et al. Spontaneous low frequency oscillations of cerebral hemodynamics and metabolism in human adults. *Neuroimage* 2000; 12: 623–639.
30. Zheng F, Sassaroli A and Fantini S. Phasor representation of oxy- and deoxyhemoglobin concentrations: what is the meaning of out-of-phase oscillations as measured by near-infrared spectroscopy?. *J Biomed Opt* 2010; 15: 40512–40513.
31. Dineen NE, Brodie FG, Robinson TG, et al. Continuous estimates of dynamic cerebral autoregulation during transient hypocapnia and hypercapnia. *J Appl Physiol* 2010; 108: 604–613.
32. Panerai RB, Dineen NE, Brodie FG, et al. Spontaneous fluctuations in cerebral blood flow regulation: contribution of PaCO₂. *J Appl Physiol* 2010; 109: 1860–1868.
33. Wagshul ME, Eide PK and Madsen JR. The pulsating brain: a review of experimental and clinical studies of intracranial pulsatility. *Fluids Barriers CNS* 2011; 8: 1–23.
34. Halliday DM, Rosenberg JR, Amjad AM, et al. A framework for the analysis of mixed time series/point process data – theory and application to the study of physiological tremor, single motor unit discharges and electromyograms. *Prog Biophys Mol Biol* 1995; 64: 237–278.
35. Bendat J and Piersol A. *Random data analysis and measurement procedures*, 4th ed. Hoboken, New Jersey: John Wiley And Sons Ltd, 2010.
36. Angleys H, Østergaard L and Jespersen SN. The effects of capillary transit time heterogeneity (CTH) on brain oxygenation. *J Cereb Blood Flow Metab* 2015; 35: 806–817.
37. Jespersen SN and Østergaard L. The roles of cerebral blood flow, capillary transit time heterogeneity, and oxygen tension in brain oxygenation and metabolism. *J Cereb Blood Flow Metab* 2012; 32: 264–277.
38. Mitsis GD, Ainslie PN, Poulin MJ, et al. Nonlinear modeling of the dynamic effects of arterial pressure and blood gas variations on cerebral blood flow in healthy humans. *Adv Exp Med Biol* 2004; 551: 259–265.
39. Panerai R, Dawson S and Potter J. Linear and nonlinear analysis of human dynamic cerebral autoregulation. *AJP Hear Circ Physiol* 1999; 277: 1089–1099.
40. Phillip D, Schytz HW, Selb J, et al. Low frequency oscillations in cephalic vessels assessed by near infrared spectroscopy. *Eur J Clin Invest* 2012; 42: 1180–1188.
41. Deegan BM, Sorond FA, Lipsitz LA, et al. Gender related differences in cerebral autoregulation in older healthy subjects. In: *Proceedings of the 31st annual international conference of the IEEE engineering in medicine and biology society: engineering the future of biomedicine, EMBC 2009*. 2009, pp.2859–2862. New York, USA: IEEE.